Crystal structure of the two-dimensional coordination polymer poly[di-μ-bromido-bis(μ-tetrahydrothiophene)dicopper(I)]

Michael Knorr,[a]* Lydie Viau,[a]* Yoann Rousselin[b] and Marek M. Kubicki[b]*

[a]Institut UTINAM UMR CNRS 6213, Université Bourgogne Franche-Comté, 16 route de Gray, 25030 Besançon, France, and [b]ICMUB UMR CNRS 6302, Université Bourgogne Franche-Comté, 9 avenue Alain Savary, 21078 Dijon, France. *Correspondence e-mail: michael.knorr@univ-fcomte.fr, lydie.viau@univ-fcomte.fr, marek.kubicki@u-bourgogne.fr

The polymeric title compound, $[Cu_2Br_2(C_4H_8S)_2]_n$, **CP1**, represents an example of a two-dimensional coordination polymer resulting from reaction of CuBr with tetrahydrothiophene (THT) in MeCN solution. The two-dimensional layers consist of two different types of rhomboid-shaped dinuclear $Cu(\mu_2\text{-Br})_2Cu$ secondary building units (SBUs); one with a quite loose Cu···Cu separation of 3.3348 (10) Å and a second one with a much closer intermetallic contact of 2.9044 (9) Å. These SBUs are interconnected through bridging THT ligands, in which the S atom acts as a four-electron donor bridging each $Cu(\mu_2\text{-Br})_2Cu$ unit in a μ_2-bonding mode. In the crystal, the layers are linked by very weak C—H···Br hydrogen bonds with H···Br distances of 2.95 Å, thus giving rise to a three-dimensional supramolecular network.

1. Chemical context

The five-membered heterocyclic ligand tetrahydrothiophene (THT) is known to form a great variety of molecular complexes and coordination polymers (CPs) with various transition metals. In addition, numerous structurally characterized examples coordinated by terminal or bridging THT ligands have been documented for the soft coinage metal ions Cu^I, Ag^I and Au^I (Usón *et al.*, 1984; Noren & Oskarsson, 1985; Mälger *et al.*, 1992; Ahrland *et al.*, 1993; López-De-Luzuriaga *et al.*, 1997; Ahrens & Jones, 2000). The research group of Pike has shown that depending on the reaction conditions, the treatment of CuI with THT affords dinuclear $[(THT)_2Cu(\mu_2\text{-}I)_2Cu(THT)_2]$, or the tetranuclear closed cubane-type cluster $[(Cu_4(\mu_3\text{-}I)_4(THT)_4]$ or $[(CuI)_{10}(THT)_7(MeCN)]_n$ (Henline *et al.*, 2014). The latter contains the mixed motif $[(Cu_4I_4(THT)](\mu_2\text{-THT})_2(Cu_2I_2)(\mu_2\text{-THT})_2[Cu_4I_4(THT)]$ held together side-by-side by two μ_2-THT assembling ligands to form a 1D ladder structure. Furthermore, the two-dimensional CP $[(CuI)_3(THT)_3\cdot MeCN]_n$ featuring a sheet structure in which $Cu_3(THT)$ rings are linked in trigonal directions by rhomboid Cu_2I_2 dimers is literature-known (Henline *et al.*, 2014). The luminescent product $[(CuI)_4(THT)_2]_n$ consisting of Cu_4I_4 cubane units knit into a 3D network by μ_2-THT ligands was also described previously (Noren & Oskarsson, 1987; Henline *et al.*, 2014). A series of solvent-dependent 2D polymers results from treatment of $[Cu(CO)Cl]_n$ with THT in THF, CH_2Cl_2 and DMF, exhibiting the composition $[(CuCl)(THT)]_n$ (THF), $[(CuCl)(THT)]_n$ (CH_2Cl_2), and $[(CuCl)_3(THT)_2]_n$
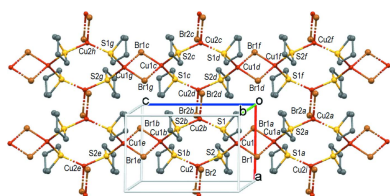
(DMF), respectively. The materials obtained in THF and CH_2Cl_2 are polymorphs (Solari *et al.*, 1996). A mono-dimensional ribbon $[(CuCl)_2(THT)_3]_n$ is generated by reaction of CuCl in neat THT (Mälger *et al.*, 1992). Even mixed-valence Cu^I/Cu^{II} compounds such as polymeric penta-μ-chloro-tris-μ-tetrahydrothiophene-tetracopper(I,II) have been observed (Ainscough *et al.*, 1985). Mälger and co-workers also showed that the treatment of CuBr in neat THT leads to the formation of a very labile rhomboid-based 1D polymer of the type $[(CuBr)_2(THT)_3]_n$ isostructural with its $[(CuCl)_2(THT)_3]_n$ analogue (Mälger *et al.*, 1992) (CSD JUDKOI).
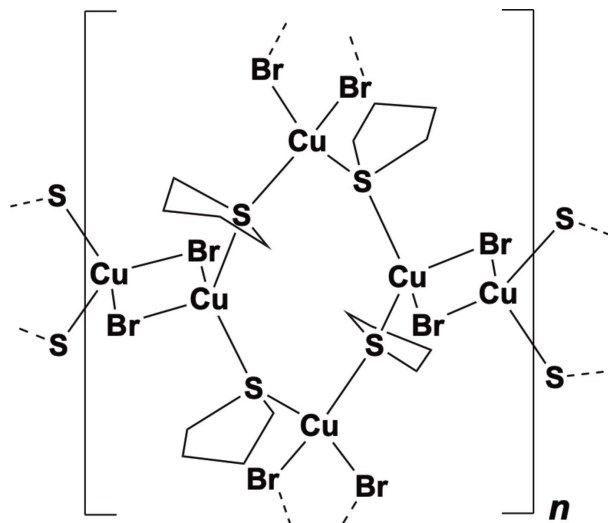
In the context of our research interest in the assembly of molecular cluster compounds and coordination polymers by complexation of dialkyl sulfides *R–S–R* or dithiolane- and dithiane-based thiaheterocycles with Cu*X* salts (Knorr *et al.*, 2010, 2015; Lapprand *et al.*, 2013; Raghuvanshi *et al.*, 2017,
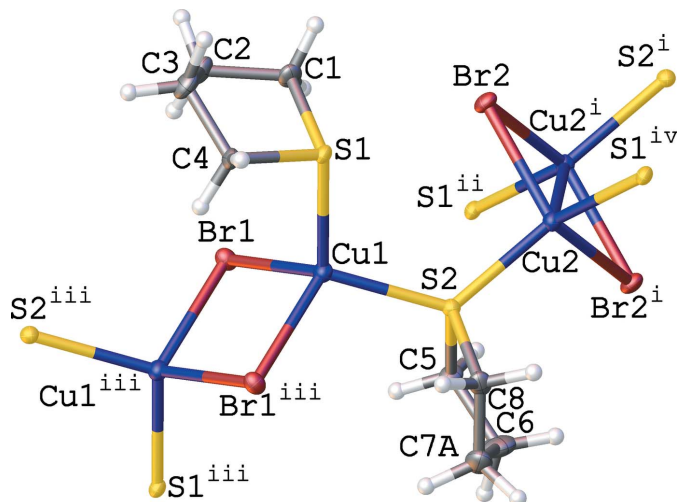
2019; Schlachter *et al.*, 2018; Knauer *et al.*, 2020), we have also investigated the complexation of CuBr by THT in acetonitrile as solvent (see Fig. 5) and present here the respective crystal structure, which differs both in composition and dimensionality (two-dimensional *vs* mono-dimensional) from the CP $[(CuBr)_2(THT)_3]_n$ reported by Mälger. Note that this colourless material crystallizes easily in the form of large well-shaped crystals that are stable in a THT-saturated environment, but decomposes rapidly by dissociation of volatile THT upon exposure to air.

2. Structural commentary

The crystal structure of **CP1** of composition $[(CuBr)_2(THT)_2]_n$ is built of $Cu(\mu_2\text{-Br})_2Cu$ rhomboids as SBUs and tetrahydrothiophene ligands. The asymmetric unit contains two independent planar Cu_2Br_2 units placed over the symmetry centres at $\frac{1}{2}, 0, 0$ $(Cu1Br1)_2$ and $1, 0, \frac{1}{2}$ $(Cu2Br2)_2$. They are connected through the sulfur atoms of thiophene ligands acting, like in all bridging monothioethers, as four-electron donors (Fig. 1). The bridging S1 atoms develop the chains of alternating $(Cu1Br1)_2$ and $(Cu2Br2)_2$ SBUs parallel to one diagonal $[\bar{1}01]$ direction of the *a0c* face of the unit cell (labelled on Fig. 2 from Cu2*h* to Cu2*i*), whereas the S2 atoms develop the analogous chains labelled from Cu2*e* to Cu2*f* parallel to the second diagonal $[101]$ direction of this face. The thus formed 2D layers lie over the (010) planes (Fig. 2). This is the essential difference from the 1D polymer $[(CuBr)_2(THT)_3]_n$ described by Mälger (Mälger *et al.*, 1992) in which only one THT molecule acts as a bridging ligand, developing a chain in one direction, whereas the two other THT molecules are terminal. The outstanding feature of the structure of **CP1** consists of largely different (0.43 Å) Cu···Cu distances in $(Cu1Br1)_2$ and $(Cu2Br2)_2$ units [3.3348 (10) Å *vs* 2.9044 (9) Å], albeit in similar chemical surroundings. Contrary to these metal-to-metal separations, the Cu—Br and Cu—S bond lengths are similar in both rhomboids. In the 1D polymer of Mälger, the Cu···Cu distance of 2.7784 (7) Å is significantly shorter than in **CP1**. Note that the presence of

Figure 1
A view of **CP1** depicting the independent Cu_2Br_2 SBUs and THT ligands. Ellipsoids are shown at the 50% probability level. Only the major component of disordered atom C7 is shown. Symmetry codes: (i) $-x + 2$, $-y$, $-z + 1$; (ii) $x + 1$, y, z;) iii) $-x + 1$, $-y$, $-z$; (iv) $-x + 1$, $-y$, $-z + 1$.
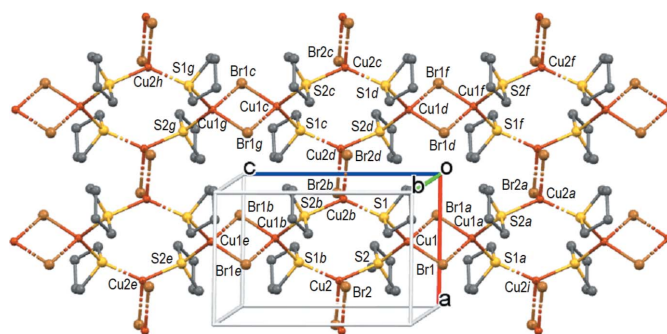
Figure 2
Projection of one layer on the *a0c* plane in the structure of **CP1**. Hydrogen atoms are omitted for clarity. Only the major component of disordered C7 atom is shown. Symmetry codes: (a) $-x + 1$, $-y$, $-z$; (b) $-x + 1$, $-y$, $-z + 1$; (c) $-x$, $-y$, $-z + 1$; (d) $x - 1$, y, z; (e) x, y, $z + 1$; (f) $-x$, $-y$, $-z$; (g) $x - 1$, y, $z + 1$; (h) $-x$, $-y$, $-z + 2$; (i) x, y, $z + 1$; (j) x, y, $z - 1$.

two independent Cu_2Br_2 SBUs has been also reported for the structure of $Cu_2Br_2(1,4\text{-oxathiane})_2$ but the difference between the Cu···Cu distances therein is equal only to 0.12 Å [2.740 (3) Å *vs* 2.865 (4) Å; Barnes & Paton, 1982; CSD BOGTIA]. This difference is still smaller in two other CPs with different Cu_2Br_2 SBUs: $[\{Cu(\mu_2\text{-Br})_2Cu\}\{\mu\text{-PhS(CH}_2)_3\text{-}SPh\}_2]_n$ [dCu···Cu = 2.794 (1) and 2.776 (1) Å; Knorr *et al.*, 2012; CSD ZEHREL] and in $[\{Cu(\mu_2\text{-Br})_2Cu\}\{\mu\text{-}p\text{-}MeC_6H_4SCH_2C\equiv CCH_2SC_6H_4Me\text{-}p]_n$ [dCu···Cu = 2.9306 (14) and 2.9662 (14) Å; Bonnot *et al.*, 2015; CSD QUPXOQ]. These observations indicate a high flexibility of the Cu_2Br_2 units. It is worth noting that the Cu···Cu distances in coordination polymers containing dibromodicopper units and bridging monothioethers have been observed in the range from 2.740 (3) Å in $Cu_2Br_2(1,4\text{-oxathiane})_2$ (Barnes & Paton, 1982) to 3.074 (1) Å at 115 K in $[(Cu_2Br_2)(Cu_4Br_4)(SMeEt)_6]_n$ (Knorr *et al.*, 2010). Thus, the Cu1··· Cu1 distance of 3.3348 (10) Å in **CP1** is the longest one observed in Cu_2Br_2 CPs with bridging monothioethers. The coordination polyhedra of the Cu1 and Cu2 atoms are best described as distorted tetrahedral. Even though the values of four-coordinate geometry τ_4 indexes of Yang (Yang *et al.*, 2007) of 0.88 support a trigonal–pyramidal geometry (theoretical values are equal to 0.85 for C_{3v} and 1.0 for T_d symmetries), the tetrahedral character THC_{DA} parameters of Höpfl (0.66 for Cu1 and 0.60 for Cu2) are closer to the tetrahedral (THC = 1.0) than pyramidal (THC = 0) geometries (Höpfl, 1999). Moreover, the sums of all six bond angles around Cu1 (656.7°) and Cu2 (656.1°) are very close to the value expected for T_d symmetry (657°) and far from that of 630° in an ideal trigonal–pyramidal geometry.

3. Supramolecular features

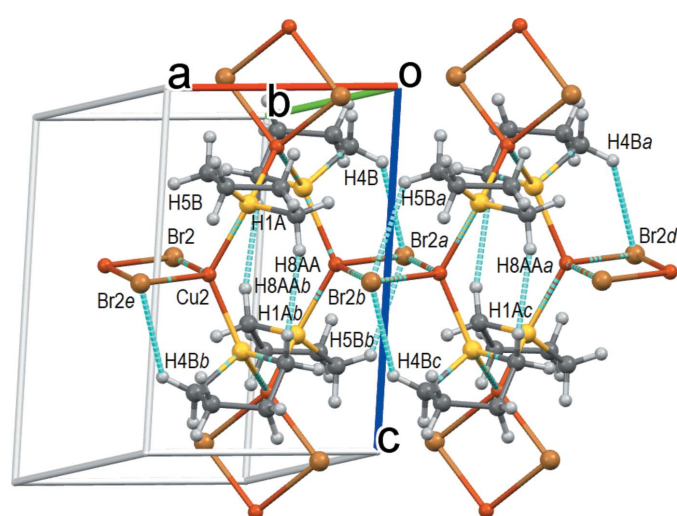The layers are built through dative Cu—S coordination bonds. There are also weak non-covalent CH···HC

Table 1
Hydrogen-bond geometry (Å, °).

D—H···A	D—H	H···A	D···A	D—H···A
C4—H4B···Br2^{iv}	0.99	2.90	3.566 (4)	125
C5—H5B···Br2^{ii}	0.99	2.89	3.556 (4)	126
C7A—H7AA···Br2^{v}	0.99	2.95	3.885 (6)	157

Symmetry codes: (ii) $-x+2, -y, -z+1$; (iv) $x-1, y, z$; (v) $x, y-1, z$.

[d(H1A···H8AA) = 2.36 Å] van der Waals contacts and C—H···Br [d(Br2···H4B) = 2.90 Å; d(Br2···H5B) = 2.89 Å] hydrogen bonds within the layers (Fig. 3 and Table 1). More interestingly, the interlayer connectivity for formation of a supramolecular 3D structure is apparently limited only to very weak C—H···Br hydrogen bonds (Fig. 4). The Br2···H7AA distance of 2.95 Å is shorter by only 0.10 Å than the sum of the van der Waals radii (Bondi, 1964). It is noteworthy that only bromine Br2 participates in hydrogen-bonding contacts and not the bromine atom Br1. In the Cu1Br1 rhomboids, the Br··· Br distance is short, the Cu···Cu distance is long and there are no Br···H bonds, while in the Cu2Br2 rhomboids the opposite is observed with long Br···Br and short Cu···Cu distances and the presence of Br2···H interactions. However, we don't believe that the presence or absence of weak hydrogen bonding alone may explain the large difference in the Cu···Cu distances.

4. Database survey

The rich structural diversity of THT-ligated molecular and polymeric copper(I) halide compounds was already laid out extensively in the *Chemical context* section above. Further examples found in a database survey using *CONQUEST* (Bruno *et al.*, 2002) comprise, for example, the three-dimensional MOF [tris(μ_2-cyano)-tris(μ_2-THT)tricopper(I)]$_n$ (CSD

Figure 3
Intralayer CH···Br and CH···HC non-covalent interactions. Symmetry codes: (a) $x-1, y, z$; (b) $-x+1, -y, -z+1$; (c) $-x, -y, -z+1$; (d) $x-2, y, z$; (e) $-x+2, -y, -z+1$.
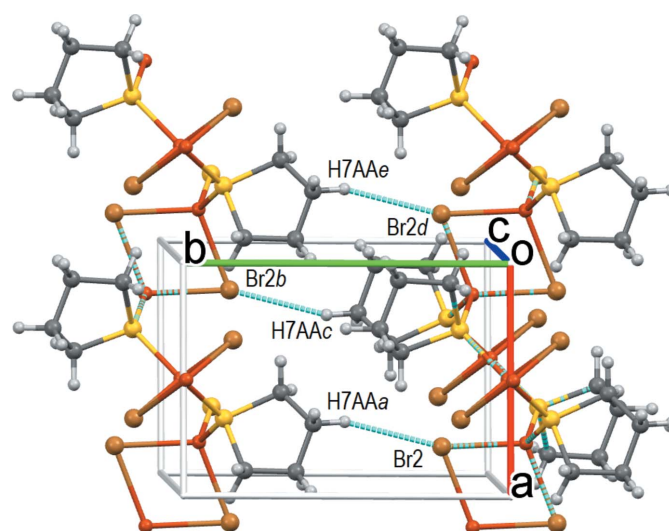

Figure 4
Interlayer CH···Br hydrogen bonds. Symmetry codes: (a) $x, y+1, z$; (b) $-x+1, -y+1, -z+1$; (c) $-x+1, -y, -z+1$; (d) $x-1, y, z$; (e) $x-1, y+1, z$.

ITEZOX), which was isolated upon treatment of CuCN with THT (Dembo *et al.*, 2010). An example of a cationic dinuclear bipyridine-bridged complex is (μ-4,4′-bipyridine)bis(THT)-tetrakis(triphenylphosphine)di-copperbis(tetrafluoroborate) (CSD MOJWOZ; Royzman *et al.*, 2014). A structurally characterized molecular organometallic aryl complex [2,6-bis(2,4,6-triisopropylphenyl)phenyl](THT)copper(I) (CSD DOPMUR) is another relevant contribution in this context (Groysman & Holm, 2009). There is also the interesting case of the tetranuclear compound *cyclo*[tetrakis(μ_2-mesityl-idene)bis(THT-copper)dicopper(I)] featuring bridging aryl groups and terminal bound THT ligands (Meyer *et al.*, 1989). For selected examples of molecular thioether-ligated complexes incorporating dinuclear Cu(μ_2-Br)$_2$Cu SBUs, see: [{Cu(μ_2-Br)$_2$Cu}{1-oxa-4,7-dithiacyclononane}$_2$] [Lucas *et al.*, 1997; CSD NONWOC, dCu$\cdots$Cu = 2.852 (2) Å]; [{Cu(μ_2-Br)$_2$Cu}{phenyl propargyl sulfide}$_4$] [Kokoli *et al.*, 2013; CSD VEQXUM, dCu$\cdots$Cu = 3.0062 (7) Å]. For selected examples of mono-dimensional thioether-assembled CPs incorporating dinuclear Cu(μ_2-Br)$_2$Cu SBUs, see: [{Cu(μ_2-Br)$_2$Cu}{μ-PhSCH$_2$SPh}$_2$]$_n$ [Knorr *et al.*, 2014; CSD FOWZIC, dCu$\cdots$Cu = 2.9192 (8) Å]; [{Cu(μ_2-Br)$_2$Cu}{μ-PhS(CH$_2$)$_3$SPh}$_2$]$_n$ [Knorr *et al.*, 2012; CSD ZEHREL, dCu$\cdots$Cu = 2.794 (1) and 2.776 (1) Å]; [Cu(μ_2-Br)$_2$Cu{μ-p-EtSCH$_2$C$_6$H$_4$C$_6$H$_4$CH$_2$SEt-p}$_2$]$_n$ [Toyota *et al.*, 1996; CSD ZARYUM01, dCu$\cdots$Cu = 2.918 (11) Å]; [Cu(μ_2-Br)$_2$Cu{μ-O$_2$S$_2$-macrocycle)$_2$]$_n$ [Park *et al.*, 2012; CSD GAXHIY, dCu$\cdots$Cu = 2.927 (1) Å].

For selected examples of two-dimensional thioether-assembled CPs incorporating dinuclear Cu(μ_2-Br)$_2$Cu SBUs, see: [{Cu$_2$(μ_2-Br)$_2$}(tetrathiaphthalazinophane)$_2$]$_n$ [Chen *et al.*, 1993; CSD HANGUY, dCu$\cdots$Cu = 3.06 (8) Å]; [{Cu(μ_2-Br)$_2$Cu}(μ_2-2-isobutyl-1,3-dithiane)$_2$]$_n$ [Raghuvanshi *et al.*, 2019; CSD JIZQOB, dCu$\cdots$Cu = 2.9057 (8) Å]; [{Cu(μ_2-Br)$_2$Cu}{μ-PhCH$_2$S(CH$_2$)$_6$SCH$_2$Ph}$_2$]$_n$ [Schlachter *et al.*, 2020; CSD IHIBUZ, dCu$\cdots$Cu = 2.953 (3) Å]; [{Cu(μ_2-Br)$_2$Cu}{μ-PhCH$_2$S(CH$_2$)$_7$SCH$_2$Ph}$_2$]$_n$ [Schlachter *et al.*, 2020; CSD IHICOU, dCu$\cdots$Cu = 2.7081 (4) Å]; [{Cu(μ_2-Br)$_2$Cu}(μ-1,2,4,5-tetramethylmercaptobenzene)]$_n$ [Suenaga *et al.*, 1997; CSD WIQMIS, dCu$\cdots$Cu = 3.1073 (12) Å]. An evaluation of these examples emphasizes that the Cu$\cdots$Cu separations within the dinuclear Cu(μ_2-Br)$_2$Cu SBUs are quite variable.
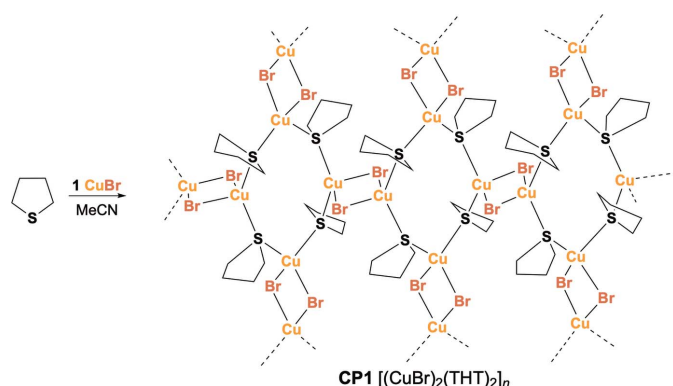
Table 2
Experimental details.

Crystal data	
Chemical formula	[Cu$_2$Br$_2$(C$_4$H$_8$S)$_2$]
M_r	463.23
Crystal system, space group	Triclinic, $P\bar{1}$
Temperature (K)	115
a, b, c (Å)	6.8076 (3), 9.7078 (4), 10.1579 (4)
α, β, γ (°)	75.804 (2), 89.845 (2), 89.594 (2)
V (Å^3)	650.79 (5)
Z	2
Radiation type	Mo $K\alpha_1$
μ (mm^{-1})	9.69
Crystal size (mm)	0.25 × 0.15 × 0.1
Data collection	
Diffractometer	Nonius Kappa APEXII
Absorption correction	Multi-scan (Blessing, 1995)
T_{min}, T_{max}	0.024, 0.072
No. of measured, independent and observed [$I > 2\sigma(I)$] reflections	5297, 2954, 2743
R_{int}	0.021
$(\sin\theta/\lambda)_{max}$ (Å^{-1})	0.651
Refinement	
$R[F^2 > 2\sigma(F^2)]$, $wR(F^2)$, S	0.030, 0.075, 1.09
No. of reflections	2954
No. of parameters	132
No. of restraints	6
H-atom treatment	H-atom parameters constrained
$\Delta\rho_{max}$, $\Delta\rho_{min}$ (e Å^{-3})	0.82, −0.91

Computer programs: *COLLECT* (Nonius, 1997), *HKL*, *DENZO* and *SCALEPACK* (Otwinowski & Minor 1997), *SIR97* (Burla *et al.*, 2007), *SHELXL2018/3* (Sheldrick, 2015) and *OLEX2* (Dolomanov *et al.*, 2009).

5. Synthesis and crystallization

To a solution of CuBr (1.43 g, 10.0 mmol) in MeCN (12 mL) was added neat THT (1.058 g, 12.0 mmol) *via* syringe. The solution turned brownish-red and a colourless microcrystalline material commenced to precipitate. The suspension was stirred at 293 K for 2 h, then heated 2 min to reflux until all product dissolved. While slowly warming to ambient temperature, colourless crystals formed progressively (Fig. 5). Filtering off the product after 1 d and storing the mother liquor in a refrigerator afforded a second crop of **CP1**. Overall yield (1.80 g, 78% yield). Calculated for C$_8$H$_{16}$Br$_2$Cu$_2$S$_2$: C, 20.74 H, 3.48; S, 13.84. Found: C, 20.35; H, 3.28, S, 13.41%.

6. Refinement

Crystal data, data collection and structure refinement details are summarized in Table 2. All H atoms were placed in calculated positions and treated with a riding model. C—H distances were set to 0.99 Å with U_{iso}(H) = $1.2U_{eq}$(C). C7 in one of the THT ligands as well as the riding methylene hydrogen atoms on C6, C7 and C8 are disordered over two locations. Their occupancy factors refined to 0.77 (1) and 0.23 (1). The disorder was modelled using a SADI constraint for the affected C—C distances.

Funding information

Figure 5
Reaction scheme for the synthesis of **CP1**.

research communications

References

Ahrens, B. & Jones, P. G. (2000). *Z. Naturforsch. Teil B*, **55**, 803–813.

Ahrland, S., Dreisch, K., Norén, B. & Oskarsson, A. (1993). *Mater. Chem. Phys.* **35**, 281–289.

Ainscough, E. W., Brodie, A. M., Husbands, J. M., Gainsford, G. J., Gabe, E. J. & Curtis, N. F. (1985). *J. Chem. Soc. Dalton Trans.* pp. 151–158.

Barnes, J. C. & Paton, J. D. (1982). *Acta Cryst.* B**38**, 3091–3093.

Blessing, R. H. (1995). *Acta Cryst.* A**51**, 33–38.

Bondi, A. (1964). *J. Phys. Chem.* **68**, 441–451.

Bonnot, A., Knorr, M., Strohmann, C., Golz, C., Fortin, D. & Harvey, P. D. (2015). *J. Inorg. Organomet. Polym.* **25**, 480–494.

Bruno, I. J., Cole, J. C., Edgington, P. R., Kessler, M., Macrae, C. F., McCabe, P., Pearson, J. & Taylor, R. (2002). *Acta Cryst.* B**58**, 389–397.

Burla, M. C., Caliandro, R., Camalli, M., Carrozzini, B., Cascarano, G. L., De Caro, L., Giacovazzo, C., Polidori, G., Siliqi, D. & Spagna, R. (2007). *J. Appl. Cryst.* **40**, 609–613.

Chen, L., Thompson, L. K., Tandon, S. & Bridson, J. N. (1993). *Inorg. Chem.* **32**, 4063–4068.

Dembo, M. D., Dunaway, L. E., Jones, J. S., Lepekhina, E. A., McCullough, S. M., Ming, J. L., Li, X., Baril-Robert, F., Patterson, H. H., Bayse, C. A. & Pike, R. D. (2010). *Inorg. Chim. Acta*, **364**, 102–114.

Dolomanov, O. V., Bourhis, L. J., Gildea, R. J., Howard, J. A. K. & Puschmann, H. (2009). *J. Appl. Cryst.* **42**, 339–341.

Groysman, S. & Holm, R. H. (2009). *Inorg. Chem.* **48**, 621–627.

Henline, K. M., Wang, C., Pike, R. D., Ahern, J. C., Sousa, B., Patterson, H. H., Kerr, A. T. & Cahill, C. L. (2014). *Cryst. Growth Des.* **14**, 1449–1458.

Höpfl, H. (1999). *J. Organomet. Chem.* **581**, 129–149.

Knauer, L., Knorr, M., Viau, L. & Strohmann, C. (2020). *Acta Cryst.* E**76**, 38–41.

Knorr, M., Bonnot, A., Lapprand, A., Khatyr, A., Strohmann, C., Kubicki, M. M., Rousselin, Y. & Harvey, P. D. (2015). *Inorg. Chem.* **54**, 4076–4093.

Knorr, M., Guyon, F., Khatyr, A., Strohmann, C., Allain, M., Aly, S. M., Lapprand, A., Fortin, D. & Harvey, P. D. (2012). *Inorg. Chem.* **51**, 9917–9934.

Knorr, M., Khatyr, A., Dini Aleo, A., El Yaagoubi, A., Strohmann, C., Kubicki, M. M., Rousselin, Y., Aly, S. M., Fortin, D., Lapprand, A. & Harvey, P. D. (2014). *Cryst. Growth Des.* **14**, 5373–5387.

Knorr, M., Pam, A., Khatyr, A., Strohmann, C., Kubicki, M. M., Rousselin, Y., Aly, S. M., Fortin, D. & Harvey, P. D. (2010). *Inorg. Chem.* **49**, 5834–5844.

Kokoli, T., Olsson, S., Björemark, P. M., Persson, S. & Håkansson, M. (2013). *J. Organomet. Chem.* **724**, 17–22.

Lapprand, A., Bonnot, A., Knorr, M., Rousselin, Y., Kubicki, M. M., Fortin, D. & Harvey, P. D. (2013). *Chem. Commun.* **49**, 8848–8850.

López-De-Luzuriaga, J.-M., Schier, A. & Schmidbaur, H. (1997). *Chem. Ber. Recl*, **130**, 647–650.

Lucas, C. R., Liang, W., Miller, D. O. & Bridson, J. N. (1997). *Inorg. Chem.* **36**, 4508–4513.

Mälger, H., Olbrich, F., Kopf, J., Abeln, D. & Weiss, E. (1992). *Z. Naturforsch. Teil B*, **47**, 1276–1280.

Meyer, E. M., Gambarotta, S., Floriani, C., Chiesi-Villa, A. & Guastini, C. (1989). *Organometallics*, **8**, 1067–1079.

Nonius (1997). *COLLECT*. Nonius BV, Delft, The Netherlands.

Norén, B. & Oskarsson, A. (1985). *Acta Chem. Scand.* **39a**, 701–709.

Norén, B. & Oskarsson, A. (1987). *Acta Chem. Scand.* **41a**, 12–17.

Otwinowski, Z. & Minor, W. (1997). *Methods in Enzymology*, Vol. 276, *Macromolecular Crystallography*, Part A, edited by C. W. Carter Jr & R. M. Sweet, pp. 307–326. New York: Academic Press.

Park, I.-H., Kim, H. J. & Lee, S. S. (2012). *CrystEngComm*, **14**, 4589–4995.

Raghuvanshi, A., Dargallay, N. J., Knorr, M., Viau, L., Knauer, L. & Strohmann, C. (2017). *J. Inorg. Organomet. Polym.* **27**, 1501–1513.

Raghuvanshi, A., Knorr, M., Knauer, L., Strohmann, C., Boullanger, S., Moutarlier, V. & Viau, L. (2019). *Inorg. Chem.* **58**, 5753–5775.

Royzman, D. E., Noviello, A. M., Henline, K. M., Pike, R. D., Killarney, J. P., Patterson, H. H., Crawford, C. & Assefa, Z. (2014). *J. Inorg. Organomet. Polym.* **24**, 66–77.

Schlachter, A., Lapprand, A., Fortin, D., Strohmann, C., Harvey, P. D. & Knorr, M. (2020). *Inorg. Chem.* **59**, 3686–3708.

Schlachter, A., Viau, L., Fortin, D., Knauer, L., Strohmann, C., Knorr, M. & Harvey, P. D. (2018). *Inorg. Chem.* **57**, 13564–13576.

Sheldrick, G. M. (2015). *Acta Cryst.* C**71**, 3–8.

Solari, E., De Angelis, S., Latronico, M., Floriani, C., Chiesi-Villa, A. & Rizzoli, C. (1996). *J. Clust Sci.* **7**, 553–566.

Suenaga, Y., Maekawa, M., Kuroda-Sowa, T., Munakata, M., Morimoto, H., Hiyama, N. & Kitagawa, S. (1997). *Anal. Sci.* **13**, 1047–1049.

Toyota, S., Matsuda, Y., Nagaoka, S., Oki, M. & Akashi, H. (1996). *Bull. Chem. Soc. Jpn*, **69**, 3115–3121.

Usón, R., Laguna, A., Laguna, M., Manzano, B. R., Jones, P. G. & Sheldrick, G. M. (1984). *J. Chem. Soc. Dalton Trans.* pp. 285–292.

Yang, L., Powell, D. R. & Houser, R. P. (2007). *Dalton Trans.* pp. 955–964.

supporting information

Crystal structure of the two-dimensional coordination polymer poly[di-*μ*-bromido-bis(*μ*-tetrahydrothiophene)dicopper(I)]

Michael Knorr, Lydie Viau, Yoann Rousselin and Marek M. Kubicki

Computing details

Data collection: *COLLECT* (Nonius, 1997); cell refinement: *HKL SCALEPACK* (Otwinowski & Minor 1997); data reduction: *HKL DENZO* and *SCALEPACK* (Otwinowski & Minor 1997); program(s) used to solve structure: *SIR97* (Burla *et al.*, 2007); program(s) used to refine structure: *SHELXL2018/3* (Sheldrick, 2015); molecular graphics: *OLEX2* (Dolomanov *et al.*, 2009); software used to prepare material for publication: *OLEX2* (Dolomanov *et al.*, 2009).

Poly[di-*μ*-bromido-bis(*μ*-tetrahydrothiophene)dicopper(I)]

Crystal data

$[Cu_2Br_2(C_4H_8S)_2]$	$Z = 2$
$M_r = 463.23$	$F(000) = 448$
Triclinic, $P\bar{1}$	$D_x = 2.364$ Mg m^{-3}
$a = 6.8076$ (3) Å	Mo $K\alpha_1$ radiation, $\lambda = 0.71073$ Å
$b = 9.7078$ (4) Å	Cell parameters from 2662 reflections
$c = 10.1579$ (4) Å	$\theta = 1.0–27.5°$
$\alpha = 75.804$ (2)°	$\mu = 9.69$ mm^{-1}
$\beta = 89.845$ (2)°	$T = 115$ K
$\gamma = 89.594$ (2)°	Prism, clear light colourless
$V = 650.79$ (5) Å^3	$0.25 \times 0.15 \times 0.1$ mm

Data collection

Nonius Kappa APEXII diffractometer	$T_{min} = 0.024$, $T_{max} = 0.072$
	5297 measured reflections
Radiation source: X-ray tube, Siemens KFF Mo 2K-180	2954 independent reflections
	2743 reflections with $I > 2\sigma(I)$
Graphite monochromator	$R_{int} = 0.021$
Detector resolution: 9 pixels mm^{-1}	$\theta_{max} = 27.6°$, $\theta_{min} = 3.0°$
φ and ω scans′	$h = -8 \rightarrow 8$
Absorption correction: multi-scan (Blessing, 1995)	$k = -12 \rightarrow 12$
	$l = -12 \rightarrow 13$

Refinement

Refinement on F^2	Primary atom site location: structure-invariant direct methods
Least-squares matrix: full	
$R[F^2 > 2\sigma(F^2)] = 0.030$	Hydrogen site location: inferred from neighbouring sites
$wR(F^2) = 0.075$	
$S = 1.09$	H-atom parameters constrained
2954 reflections	$w = 1/[\sigma^2(F_o^2) + (0.0333P)^2 + 2.0511P]$
132 parameters	where $P = (F_o^2 + 2F_c^2)/3$
6 restraints	$(\Delta/\sigma)_{max} < 0.001$

$\Delta\rho_{max} = 0.82$ e Å⁻³

$\Delta\rho_{min} = -0.91$ e Å⁻³

Special details

Geometry. All esds (except the esd in the dihedral angle between two l.s. planes) are estimated using the full covariance matrix. The cell esds are taken into account individually in the estimation of esds in distances, angles and torsion angles; correlations between esds in cell parameters are only used when they are defined by crystal symmetry. An approximate (isotropic) treatment of cell esds is used for estimating esds involving l.s. planes.

Fractional atomic coordinates and isotropic or equivalent isotropic displacement parameters (Å²)

	x	*y*	*z*	U_{iso}*/U_{eq}	Occ. (<1)
Br1	0.66540 (5)	0.15468 (4)	−0.03837 (3)	0.01461 (10)	
Br2	0.83088 (5)	0.17939 (4)	0.45014 (4)	0.01506 (10)	
Cu1	0.51313 (7)	−0.00292 (5)	0.16455 (5)	0.01505 (11)	
Cu2	0.82082 (6)	−0.08288 (5)	0.51958 (4)	0.01385 (11)	
S1	0.31065 (12)	0.13645 (9)	0.26538 (8)	0.01195 (17)	
S2	0.70032 (12)	−0.14665 (9)	0.33197 (9)	0.01222 (17)	
C1	0.4015 (6)	0.3198 (4)	0.2177 (4)	0.0192 (8)	
H1A	0.375096	0.368406	0.290963	0.023*	
H1B	0.544740	0.320766	0.200413	0.023*	
C2	0.2910 (6)	0.3928 (4)	0.0890 (4)	0.0206 (8)	
H2A	0.354608	0.371724	0.008315	0.025*	
H2B	0.289017	0.496987	0.077765	0.025*	
C3	0.0821 (6)	0.3339 (4)	0.1059 (4)	0.0226 (8)	
H3A	0.010384	0.370283	0.175423	0.027*	
H3B	0.009678	0.363357	0.018959	0.027*	
C4	0.0989 (6)	0.1729 (4)	0.1496 (4)	0.0163 (7)	
H4A	0.121252	0.132901	0.069998	0.020*	
H4B	−0.022152	0.131202	0.196654	0.020*	
C5	0.9163 (6)	−0.2030 (4)	0.2504 (4)	0.0179 (7)	
H5A	0.902627	−0.175035	0.150356	0.022*	
H5B	1.036738	−0.159227	0.275978	0.022*	
C6	0.9258 (7)	−0.3639 (5)	0.3012 (5)	0.0325 (10)	
H6AA	1.003988	−0.405261	0.237893	0.039*	0.771 (13)
H6AB	0.988725	−0.390717	0.391775	0.039*	0.771 (13)
H6BC	0.911154	−0.407662	0.223452	0.039*	0.229 (13)
H6BD	1.055839	−0.392163	0.342976	0.039*	0.229 (13)
C7A	0.7197 (8)	−0.4183 (6)	0.3098 (6)	0.0265 (16)	0.771 (13)
H7AA	0.716201	−0.518002	0.364131	0.032*	0.771 (13)
H7AB	0.669637	−0.415264	0.217672	0.032*	0.771 (13)
C7B	0.7690 (16)	−0.4178 (16)	0.4028 (15)	0.016 (5)*	0.229 (13)
H7BA	0.732673	−0.515246	0.398840	0.019*	0.229 (13)
H7BB	0.819357	−0.422099	0.495122	0.019*	0.229 (13)
C8	0.5925 (6)	−0.3246 (4)	0.3767 (4)	0.0188 (8)	
H8AA	0.591371	−0.362462	0.476472	0.023*	0.771 (13)
H8AB	0.455767	−0.321214	0.343042	0.023*	0.771 (13)
H8BC	0.508814	−0.337978	0.458646	0.023*	0.229 (13)
H8BD	0.513653	−0.342444	0.300886	0.023*	0.229 (13)

Atomic displacement parameters (Å²)

	U^{11}	U^{22}	U^{33}	U^{12}	U^{13}	U^{23}
Br1	0.01355 (17)	0.01735 (19)	0.01357 (17)	−0.00288 (13)	0.00077 (13)	−0.00496 (14)
Br2	0.01333 (17)	0.01052 (18)	0.02045 (19)	0.00292 (13)	−0.00208 (13)	−0.00219 (14)
Cu1	0.0167 (2)	0.0148 (2)	0.0137 (2)	0.00320 (17)	−0.00176 (16)	−0.00354 (17)
Cu2	0.0162 (2)	0.0132 (2)	0.0120 (2)	0.00180 (17)	−0.00123 (16)	−0.00298 (17)
S1	0.0142 (4)	0.0100 (4)	0.0108 (4)	0.0027 (3)	−0.0016 (3)	−0.0010 (3)
S2	0.0140 (4)	0.0111 (4)	0.0119 (4)	0.0016 (3)	−0.0012 (3)	−0.0037 (3)
C1	0.0254 (19)	0.0107 (18)	0.0198 (18)	−0.0041 (15)	−0.0019 (15)	−0.0003 (14)
C2	0.0212 (19)	0.0146 (19)	0.0218 (19)	0.0013 (15)	−0.0009 (15)	0.0036 (15)
C3	0.0189 (18)	0.018 (2)	0.027 (2)	0.0055 (15)	−0.0040 (16)	0.0000 (16)
C4	0.0198 (17)	0.0151 (18)	0.0138 (16)	0.0055 (14)	−0.0060 (14)	−0.0030 (14)
C5	0.0190 (18)	0.0183 (19)	0.0159 (17)	0.0070 (14)	0.0055 (14)	−0.0033 (14)
C6	0.038 (3)	0.021 (2)	0.041 (3)	0.0089 (19)	0.007 (2)	−0.012 (2)
C7A	0.036 (3)	0.018 (3)	0.028 (3)	−0.002 (2)	−0.010 (2)	−0.009 (2)
C8	0.0243 (19)	0.0141 (19)	0.0171 (17)	−0.0067 (15)	−0.0020 (15)	−0.0018 (14)

Geometric parameters (Å, º)

Br1—Cu1	2.4755 (6)	C3—C4	1.520 (5)
Br1—Cu1[i]	2.5000 (6)	C4—H4A	0.9900
Br2—Cu2[ii]	2.5349 (6)	C4—H4B	0.9900
Br2—Cu2	2.4711 (6)	C5—H5A	0.9900
Cu1—Cu1[i]	3.3348 (10)	C5—H5B	0.9900
Cu1—S1	2.3292 (9)	C5—C6	1.522 (6)
Cu1—S2	2.2991 (10)	C6—H6AA	0.9900
Cu2—Cu2[ii]	2.9044 (9)	C6—H6AB	0.9900
Cu2—S1[iii]	2.2982 (9)	C6—H6BC	0.9900
Cu2—S2	2.2983 (9)	C6—H6BD	0.9900
S1—C1	1.837 (4)	C6—C7A	1.497 (7)
S1—C4	1.840 (4)	C6—C7B	1.488 (12)
S2—C5	1.831 (4)	C7A—H7AA	0.9900
S2—C8	1.833 (4)	C7A—H7AB	0.9900
C1—H1A	0.9900	C7A—C8	1.526 (6)
C1—H1B	0.9900	C7B—H7BA	0.9900
C1—C2	1.523 (5)	C7B—H7BB	0.9900
C2—H2A	0.9900	C7B—C8	1.484 (12)
C2—H2B	0.9900	C8—H8AA	0.9900
C2—C3	1.530 (5)	C8—H8AB	0.9900
C3—H3A	0.9900	C8—H8BC	0.9900
C3—H3B	0.9900	C8—H8BD	0.9900
Cu1—Br1—Cu1[i]	84.167 (19)	S1—C4—H4A	110.7
Cu2—Br2—Cu2[ii]	70.916 (19)	S1—C4—H4B	110.7
Br1—Cu1—Br1[i]	95.832 (19)	C3—C4—S1	105.3 (3)
S1—Cu1—Br1	107.82 (3)	C3—C4—H4A	110.7
S1—Cu1—Br1[i]	114.58 (3)	C3—C4—H4B	110.7

S2—Cu1—Br1	121.51 (3)	H4A—C4—H4B	108.8
S2—Cu1—Br1ⁱ	108.88 (3)	S2—C5—H5A	110.6
S2—Cu1—S1	108.12 (3)	S2—C5—H5B	110.6
Br2—Cu2—Br2ⁱⁱ	109.084 (19)	H5A—C5—H5B	108.7
Br2ⁱⁱ—Cu2—Cu2ⁱⁱ	53.516 (16)	C6—C5—S2	105.7 (3)
Br2—Cu2—Cu2ⁱⁱ	55.568 (17)	C6—C5—H5A	110.6
S1ⁱⁱⁱ—Cu2—Br2	105.18 (3)	C6—C5—H5B	110.6
S1ⁱⁱⁱ—Cu2—Br2ⁱⁱ	104.86 (3)	C5—C6—H6AA	110.2
S1ⁱⁱⁱ—Cu2—Cu2ⁱⁱ	116.52 (3)	C5—C6—H6AB	110.2
S2—Cu2—Br2	104.11 (3)	C5—C6—H6BC	109.3
S2—Cu2—Br2ⁱⁱ	105.71 (3)	C5—C6—H6BD	109.3
S2—Cu2—Cu2ⁱⁱ	116.35 (3)	H6AA—C6—H6AB	108.5
S2—Cu2—S1ⁱⁱⁱ	127.13 (4)	H6BC—C6—H6BD	108.0
Cu2ⁱⁱⁱ—S1—Cu1	128.70 (4)	C7A—C6—C5	107.7 (4)
C1—S1—Cu1	108.21 (14)	C7A—C6—H6AA	110.2
C1—S1—Cu2ⁱⁱⁱ	111.26 (13)	C7A—C6—H6AB	110.2
C1—S1—C4	94.46 (18)	C7B—C6—C5	111.5 (6)
C4—S1—Cu1	102.71 (12)	C7B—C6—H6BC	109.3
C4—S1—Cu2ⁱⁱⁱ	105.46 (13)	C7B—C6—H6BD	109.3
Cu2—S2—Cu1	125.08 (4)	C6—C7A—H7AA	110.0
C5—S2—Cu1	107.52 (13)	C6—C7A—H7AB	110.0
C5—S2—Cu2	104.92 (13)	C6—C7A—C8	108.3 (4)
C5—S2—C8	93.98 (19)	H7AA—C7A—H7AB	108.4
C8—S2—Cu1	108.84 (13)	C8—C7A—H7AA	110.0
C8—S2—Cu2	111.74 (13)	C8—C7A—H7AB	110.0
S1—C1—H1A	110.6	C6—C7B—H7BA	109.4
S1—C1—H1B	110.6	C6—C7B—H7BB	109.4
H1A—C1—H1B	108.7	H7BA—C7B—H7BB	108.0
C2—C1—S1	105.9 (3)	C8—C7B—C6	111.0 (9)
C2—C1—H1A	110.6	C8—C7B—H7BA	109.4
C2—C1—H1B	110.6	C8—C7B—H7BB	109.4
C1—C2—H2A	110.5	S2—C8—H8AA	110.4
C1—C2—H2B	110.5	S2—C8—H8AB	110.4
C1—C2—C3	106.3 (3)	S2—C8—H8BC	111.3
H2A—C2—H2B	108.7	S2—C8—H8BD	111.3
C3—C2—H2A	110.5	C7A—C8—S2	106.8 (3)
C3—C2—H2B	110.5	C7A—C8—H8AA	110.4
C2—C3—H3A	110.3	C7A—C8—H8AB	110.4
C2—C3—H3B	110.3	C7B—C8—S2	102.3 (6)
H3A—C3—H3B	108.5	C7B—C8—H8BC	111.3
C4—C3—C2	107.3 (3)	C7B—C8—H8BD	111.3
C4—C3—H3A	110.3	H8AA—C8—H8AB	108.6
C4—C3—H3B	110.3	H8BC—C8—H8BD	109.2
Cu1—S1—C1—C2	91.5 (3)	S2—C5—C6—C7B	−3.4 (8)
Cu1—S1—C4—C3	−123.6 (2)	C1—S1—C4—C3	−13.8 (3)
Cu1—S2—C5—C6	−128.8 (3)	C1—C2—C3—C4	−49.3 (4)
Cu1—S2—C8—C7A	103.2 (3)	C2—C3—C4—S1	37.6 (4)

Cu1—S2—C8—C7B	143.3 (6)	C4—S1—C1—C2	−13.4 (3)
Cu2ⁱⁱⁱ—S1—C1—C2	−121.9 (2)	C5—S2—C8—C7A	−6.8 (3)
Cu2ⁱⁱⁱ—S1—C4—C3	99.7 (3)	C5—S2—C8—C7B	33.3 (6)
Cu2—S2—C5—C6	96.1 (3)	C5—C6—C7A—C8	−45.0 (5)
Cu2—S2—C8—C7A	−114.6 (3)	C5—C6—C7B—C8	30.0 (12)
Cu2—S2—C8—C7B	−74.5 (6)	C6—C7A—C8—S2	30.3 (5)
S1—C1—C2—C3	37.0 (4)	C6—C7B—C8—S2	−40.9 (11)
S2—C5—C6—C7A	38.3 (4)	C8—S2—C5—C6	−17.7 (3)

Symmetry codes: (i) −*x*+1, −*y*, −*z*; (ii) −*x*+2, −*y*, −*z*+1; (iii) −*x*+1, −*y*, −*z*+1.

Hydrogen-bond geometry (Å, º)

D—H···*A*	*D*—H	H···*A*	*D*···*A*	*D*—H···*A*
C4—H4*B*···Br2ⁱᵛ	0.99	2.90	3.566 (4)	125
C5—H5*B*···Br2ⁱⁱ	0.99	2.89	3.556 (4)	126
C7*A*—H7*AA*···Br2ᵛ	0.99	2.95	3.885 (6)	157

Symmetry codes: (ii) −*x*+2, −*y*, −*z*+1; (iv) *x*−1, *y*, *z*; (v) *x*, *y*−1, *z*.